

Elastic rotational restraint of web-post in cellular beams with sinusoidal openings

Sébastien Durif^{1,2a}, Abdelhamid Bouchaïr^{*1,2} and Claude Bacconnet^{1,2b}

¹ Clermont Université, Université Blaise Pascal, Institut Pascal, BP 10448, F-63000 Clermont-Ferrand, France
² CNRS, UMR 6602, Institut Pascal, F-63171 Aubière, France

(Received August 02, 2012, Revised June 13, 2014, Accepted June 29, 2014)

Abstract. Experimental tests on cellular beams with sinusoidal openings showed two main failure modes around the openings. They concern the formation of four plastic hinges and the local instability of the sinusoidal part of the opening. In parallel, numerical analysis of the sinusoidal part of the opening revealed the existence of an elastic rotational restraint between the intermediate web-post and the adjacent opening panel. The aim of the present study is to present an approach to quantify this rotational restraint. Through the response surface method, a mathematical model is proposed. It shows a great ability to predict the rotational restraint value as a function of the geometrical parameters of the opening. This model can be used to perform an extensive study with various geometrical configurations of beams with the aim to develop a reliable and realistic analytical model predicting the resistance of the sinusoidal openings.

Keywords: cellular beams; sinusoidal openings; local instability; elastic rotational restraint; response surface method; mathematical model

1. Introduction

Cellular beams are nowadays widely used in steel construction, especially for their high mechanical performances on long span structures. Furthermore, conducts and services can pass through the holes which reduces the floor depth (Lawson and Hicks 2005, Veljkovic *et al.* 2006). However, their mechanical behavior is different from that of normal beams. The existence of openings implies specific failure modes in addition to the common solid web beams. The main specific failure modes reported by various authors (Kerdal and Nethercot 1984, Gandomi *et al.* 2011, Lagaros *et al.* 2008), for castellated or cellular beams are the Vierendeel mechanism, the welded joint rupture in the web, the web-post shear buckling, the web-post compression buckling and the Tee compression buckling.

Those specific modes define the local failures that can appear around an opening. In the zones of high shear internal forces, the transfer of these forces around the openings implies two main local failure modes (see Fig. 1): the Vierendeel mechanism (Redwood 1978) and the web-post

*Corresponding author, Professor, E-mail: abdelhamid.bouchair@univ-bpclermont.fr

^a Ph.D., E-mail: sebastien.durif@univ-bpclermont.fr

^b Associate Professor, E-mail: claudio.bacconnet@univ-bpclermont.fr

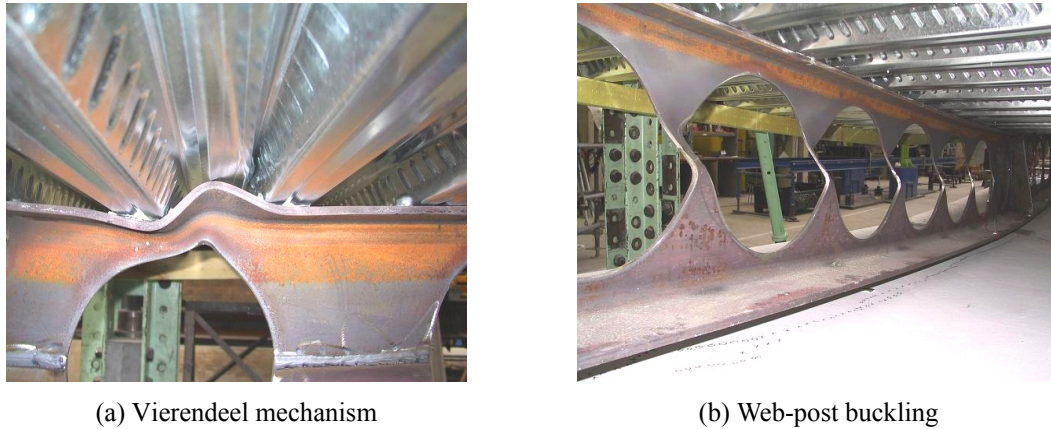


Fig. 1 Failure modes of composite cellular beams

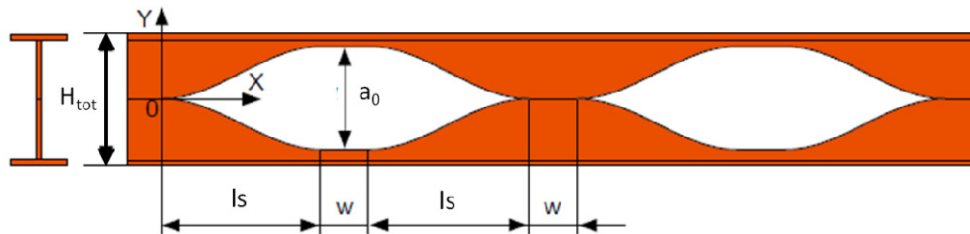


Fig. 2 Common opening shapes of cellular beams (hexagonal, circular and sinusoidal)

buckling (considering sufficient lateral bracing against global lateral-torsional buckling) (Nadjai *et al.* 2007, Soltani *et al.* 2012). Many researches have been performed in order to develop reliable and realistic design methods for those specific failure modes (Chung *et al.* 2001, ENV 1993-1-1 1995). The design methods are based on some common mechanical approaches briefly described in this paper (see part 2).

The design methods knew various evolutions to take into account the specific mechanical behavior associated to the shapes of openings. Currently, architectural and technical demands led to develop a new opening shape, the sinusoidal openings (Fig. 2). As common cellular beams (hexagonal and circular), it is made from hot rolled profiles with regular openings. Besides its esthetical advantages, this innovative shape offers a wider range of opening sizes in comparison with circular openings.

The sinusoidal shape function of the opening in the AngelinaTM beam is given by Eq. (1) considering the geometrical parameters defined in Fig. 2.

$$y = \left(0.5 \times \frac{a_0}{2}\right) \times \sin \left[\pi \times \left(\frac{x}{l_s} + \frac{3}{2} \right) \right] + \frac{a_0}{4} \quad (1)$$

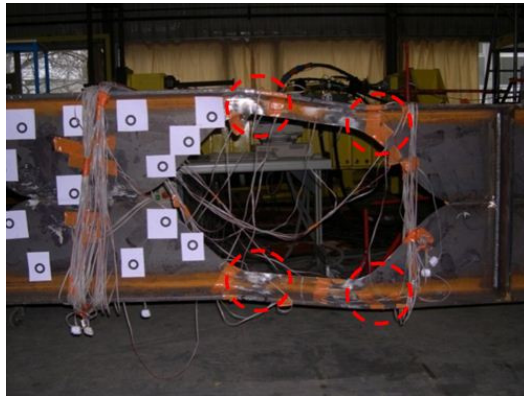
The research led on the development of new opening shapes in cellular beams showed that changing the opening shape influences the mechanical behavior of the cellular beam (Tsavdaridis 2010). The sinusoidal opening influences the behavior of the beam, especially the local failure

mode around the openings which appeared to be different from those observed on cellular beams with circular or hexagonal openings (Durif *et al.* 2013a). To study the behavior of the beams with sinusoidal openings, experimental tests were performed by the authors at Blaise Pascal University on full scale cellular beams with sinusoidal openings (Durif 2012, Durif *et al.* 2013b). As the global lateral torsional buckling was prevented, the tests showed that the main failure mode of this type of beam is linked to the Vierendeel mechanism. The failure is characterized either by the formation of four plastic hinges similarly to a rectangular or hexagonal opening (Fig. 3(a)), or by the local buckling of the compressed sinusoidal parts of the most stressed opening (Fig. 3(b)).

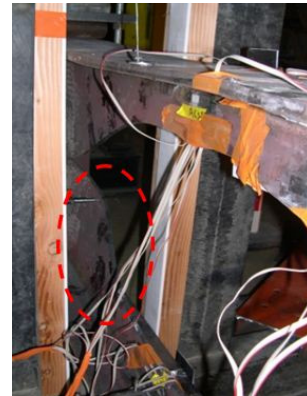
In the cellular beams with sinusoidal openings, by opposition to circular openings, the web-post is enough large to avoid the web-post shear buckling generated by the horizontal shear force. However, the length of the sinusoidal opening implies large sinusoidal panels around the opening. Thus, local buckling can arise in the sinusoidal part close to the intermediate web-post in association with the Vierendeel mechanism (see Fig. 3(b)). In this case, the intermediate web-post provides a kind of out of plan and rotational elastic support influencing the local buckling of the adjacent sinusoidal panel.

In order to analyze the local buckling of the panels around the opening due to shear force, isolated web-post is studied (Durif *et al.* 2013a). The principle of the isolated specimen, representing two tested quarters of opening, is shown in Fig. 4.

The study led by the authors showed that the two isolated quarters of opening tested in bending are appropriate to illustrate the behavior of a full scale beam considering the Vierendeel bending



(a) Formation of 4 plastic hinges (Vierendeel bending)



(b) Local buckling of the opening sinusoidal panel

Fig. 3 Failure modes of a sinusoidal opening due to local bending (Durif *et al.* 2013b)

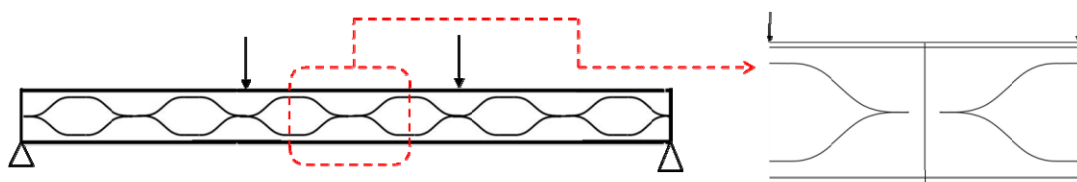


Fig. 4 Parent cellular beam and the corresponding isolated web-post specimen

including the local buckling of the sinusoidal panel (Durif *et al.* 2013a). With the isolated web-post specimen, the loading system and the internal forces in the panels are well known during the test, in comparison with the whole beam. Thus it allows studying only the influence of the geometrical parameters on the panel stiffness without varying the loading system. Besides, a numerical model was developed using the finite element software CAST3M (CEA 2012) and validated on the experimental results (Durif *et al.* 2013a).

The validated numerical model is used in this paper as a basis for a parametric study to evaluate the rotational restraint effect of the web-post on the buckling of the sinusoidal panel.

In fact, the local buckling is difficult to predict analytically and depends on the boundary conditions of the studied panels. The aim of this study is to propose a method enabling to characterize the behavior of sinusoidal openings in accordance with common analytical approaches for cellular beams. This is done by decomposing the opening in quarters and isolated web-posts. This paper aims to understand the buckling of the panels around the sinusoidal openings taking into account realistic boundary conditions. Thus, an approach based on design of experiments is proposed to point out and quantify the partial restraint provided by the intermediate web-post to the adjacent opening panel (k_θ in Fig. 9).

The parametric study is performed on selected geometries of specimens. Then, through the response surface method (Balasubramanian *et al.* 2008a, 2008b, Le 2012), a mathematical model is developed to predict the rotational restraint provided by the intermediate web-post to the adjacent opening panel.

2. Analytical models for cellular beams

The cellular beams are commonly considered as Vierendeel beams (Darwin 2003). The analytical models proposed to predict the strength of cellular beams are mainly based on the evaluation of the stresses induced by Vierendeel bending around each opening (Lawson *et al.* 2006, Tsavdaridis *et al.* 2011). Two common approaches are generally used. The first simplistic approach considers an equivalent rectangular opening and evaluates its resistance (Redwood 1978). This approach underestimates in many cases the load carrying capacities of cellular beams. The second approach considers the circular shape of the opening and checks the resistance of all the inclined Tee sections around it. Considering the Vierendeel beam equivalence, the global moment and shear force in each opening position are distributed as internal forces on the upper and the lower Tee sections of the opening (Fig. 5) (Chung *et al.* 2001).

At the mid-length of the opening, the two Tee sections are defined as Top and Bottom. In these sections the shear and the normal forces without bending moment (Vierendeel equivalence) are known. Then the internal forces (M_φ , N_φ and V_φ) are calculated in the centroid of each inclined Tee section and the resistance checked. The internal local bending in the inclined Tee-section is due to the action of normal and shear forces applied at the mid-length of the opening (Fig. 5).

This method shows a good accuracy in the prediction of the opening resistance (Ward 1990, Tsavdaridis and D'Mello 2011). For symmetrical profiles, the normal and shear internal forces applied at the mid-length of the opening can be calculated using the Eqs. (2) and (3).

$$N_{T,bot} = N_{T,top} = M_{Ed} / d_G \quad (2)$$

$$V_{Ed,T} = V_{Ed} / 2 \quad (3)$$

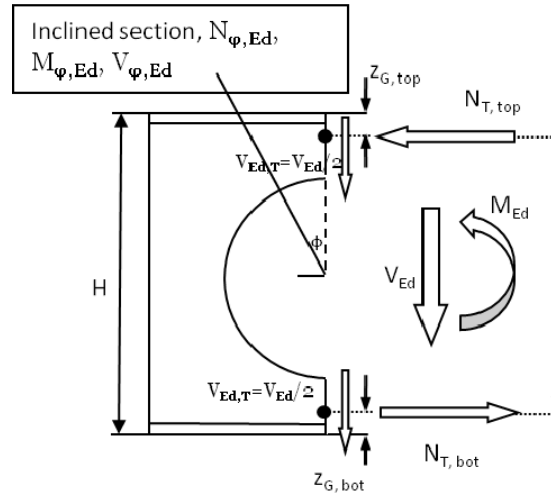


Fig. 5 Internal forces distribution around an opening of cellular beam

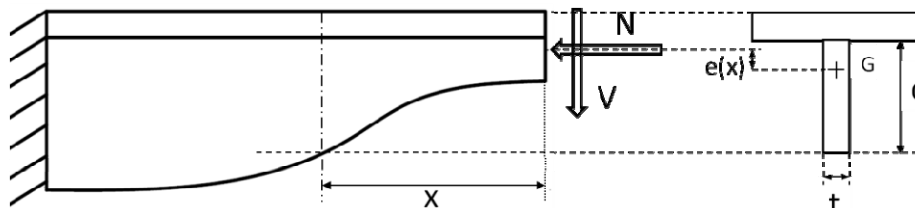


Fig. 6 Equivalent internal loads on a quarter of sinusoidal opening

where M_{Ed} is the global bending moment and V_{Ed} is the global shear force at the considered opening.

The internal forces in each inclined Tee section, defined by the angle φ , are calculated according to Fig. 5. The internal forces in the inclined sections are given by Eqs. (4) to (6) in the case of the top quarter of the opening (Fig. 5) (Tsavdaridis 2010).

$$N_{\varphi,Ed} = N_{T,top} \times \cos(\varphi) + V_{Ed} \times \sin(\varphi) \tag{4}$$

$$V_{\varphi,Ed} = N_{T,top} \times \sin(\varphi) - V_{Ed,T} \times \cos(\varphi) \tag{5}$$

$$M_{\varphi,Ed} = V_{Ed,T} \times u - N_{T,top} \times v \tag{6}$$

These applied internal forces are compared to the resistance of the inclined section. Where u and v are the horizontal and the vertical distances between the centroids of the two cross-sections at the angles 0 and φ . In order to calculate the resistance of circular openings, the common approach considers empirical formulas that allow justifying the plastic or the elastic resistance of each inclined tee sections.

To keep the same approach for the sinusoidal opening, an adaptation is performed (Fig. 6)

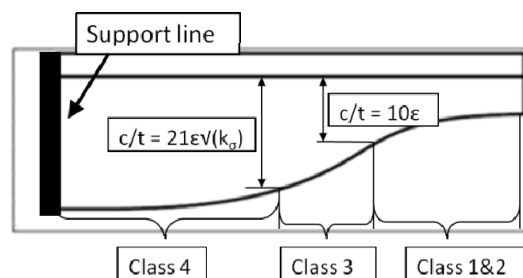


Fig. 7 Classification of the web panel Tee cross sections along a quarter of opening

considering the local internal forces in the opening quarter. In this approach, the Tee sections are not easy to define in comparison with the circular openings.

Thus, to keep an approach close to the principles of Eurocodes and as simplification, it is proposed to consider Tee sections perpendicular to the beam flanges. As a consequence, for a section located at the abscissa x , the local Vierendeel bending $M_V(x)$ can be calculated according to the Eq. (7).

$$M_V(x) = V \times x - N \times e(x) \quad (7)$$

where $e(x)$ is the distance between the centroids of the Tee sections in the mid-length of the opening and at the abscissa x . The analytical model is based on the verification of the resistance for each Tee section defined by the abscissa x .

The main challenge is to define each Tee-section resistance. Empirical methods have been developed for circular openings and do not exist for this new opening shape (ENV 1993-1-1 1995). The variation of the Tee heights along the opening length implies different Tee web slenderness. The resistance of a Tee section is based on its yielding capacity eventually reduced by the effect of local buckling. The common approaches to define the resistance of a section are based on their buckling resistances. Therefore the actual Eurocode design methods are based on the classification of section defined regarding the ratio between the height and the thickness of the compressed panel. This classification defines the yielding capacity of a Tee section. The application of the Eurocode 3 design rules gives the $c(x)/t$ limits defining the class sections and as a consequence the yielding capacity of each Tee section along the quarter (see Figs. 6 and 7) (EN 1993-1-1 2003). For class 1 and 2 sections, the tee section resistance can reach the plastic strength, whereas for class 3 sections, the resistance is limited to the elastic strength. However, for class 4 sections in which local buckling occurs before reaching the yield limit, effective widths are used to make the necessary allowances for reductions in resistance due to the effects of local buckling.

It can be seen in Fig. 7 that the major parts of the Tee sections are of class 4 (with reduced bending resistance due to local buckling). Consequently the instability is dominant in those sections. The Eurocode criteria are based on the calculation of the critical stress coefficient k_σ (Johansson *et al.* 2007). This coefficient should consider the rate of stress of the section and the boundary conditions. However, the existing design rules do not consider the specific boundary conditions of the cross-sections along a sinusoidal opening quarter. Therefore, the adaptation of those design rules to this specific case leads to very conservative results and non-realistic failure modes (Durif 2012).

Through the study led in this paper, the existence of a rotational elastic restraint provided by

the intermediate web-post on the adjacent opening quarter is shown (see Fig. 9). This rotational restraint influences the stiffness of the opening panel that could justify different classification of the cross-sections along the opening quarter, especially for the sections of maximum ratio c/t close to the intermediate web-post.

Therefore the boundary conditions are influent in the resistance of those sections. Thus it is of interest to focus on the characterization of the restraint conditions around those sections in order to define realistic stiffness and resistance.

3. Numerical analysis of the web-post restraint on the adjacent opening

3.1 Elastic rotational restraint emphasis

The previous experimental studies led on full scale cellular beams validate a finite element model developed using the software SAFIR (Durif *et al.* 2013b). This numerical model uses shell elements and makes non-linear calculations considering high displacement, and both material and geometrical non-linearities. This numerical model allows observing the influence of the rotational restraint between the intermediate web-post and the adjacent opening quarter on the buckling of the sinusoidal panel.

Considering a study in the elastic range, to avoid any influence of local plastification, the evolution of the equivalent von Mises stress (where the compressive stress is dominant) has been observed in the element with maximum out of plan displacement. This observation in the most stressed zone of whole beam is compared with the cases of two isolated opening quarters loaded by corresponding internal forces deduced from the parent cellular beam. Those two isolated specimens representing the same opening quarter are modeled considering two different edge supports (pinned or fixed). Thus, three different conditions of rotational restraint are considered between the intermediate web-post and the opening quarter (pinned, fixed or elastic) (see Fig. 8).

All the three geometries have been meshed using shell elements. The calculation has been led by increasing proportionally the axial and the shear forces until the failure. In all cases, the von

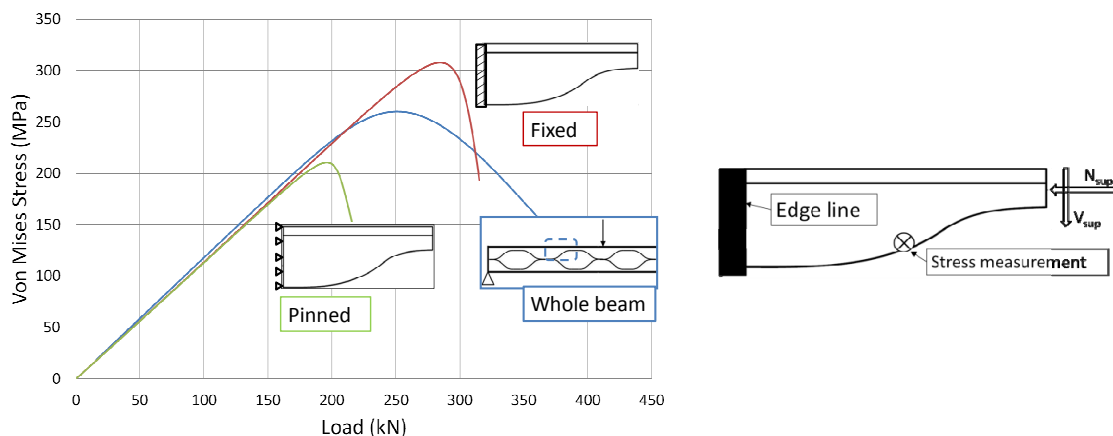


Fig. 8 Equivalent stress in three quarter panels: in whole beam (partial restraint) and isolated (pinned or fixed supports)

Mises stress is observed on the point where the maximum out of plan displacement in the whole parent cellular beam is observed. The same positions are kept for the isolated quarters (see Fig. 8 right). In order to study specifically the local buckling without any yielding, the models have been performed in pure elastic range. Thus, the descending branch of the curves is linked to the out of plan displacements of the studied elements. Fig. 8 compares the evolutions of the von Mises stress, in compressed zone, for the studied panels with three different conditions of rotational restraint between the web-post and the panel.

It can be observed that the equivalent stress in the section taken from the whole beam reaches a state of stress between both pinned and fixed conditions. Thus, the boundary condition at the edge line of the isolated quarter has clearly an influence on the sinusoidal panel stiffness. The whole beam corresponds to a case of isolated quarter with partial rotational restraint at the support (see Fig. 9). It is proposed in this study to represent the rotational restraint through an elastic rotational restraint coefficient k_θ described in Fig. 9.

Considering these observations, it seems necessary to evaluate this elastic rotational restraint at the support of the opening quarter. The aim is to represent the real behavior of the equivalent quarter observed in the whole beam. Thus, an approach is proposed to quantify the semi-rigidity (rotational restraint) provided by the intermediate web-post to the quarter of opening.

However, as the internal loads are not well known in the whole cellular beam, the study is focused on the isolated web-post with two quarters loaded in shear and bending (Fig. 10(a)). The advantage of this type of specimen used in tests is that its applied load is well defined and the internal forces are easy to calculate analytically while being close to the Vierendeel bending. Furthermore, on the basis of experimental and numerical studies (Durif *et al.* 2013a), the authors

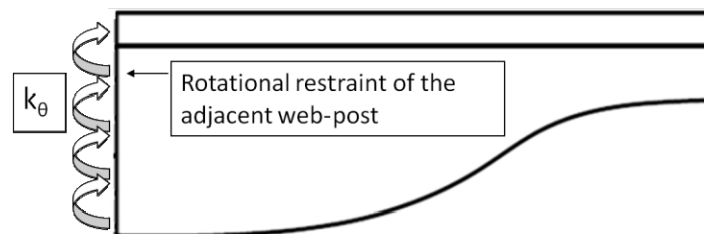


Fig. 9 Model of quarter with elastic rotational support (coefficient k_θ)

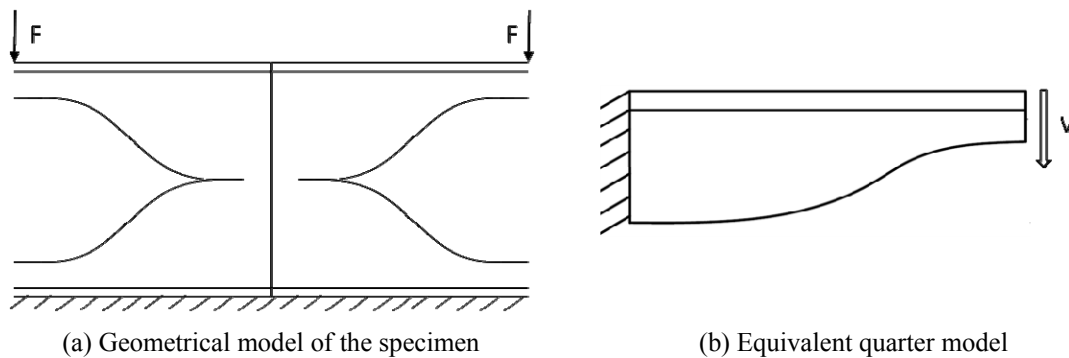


Fig. 10 Opening quarter loaded by a shear force

showed that this specimen represents well the local buckling of the opening quarter due to Vierendeel bending.

As a consequence, this specimen is used as a basis for the parametrical study led in this paper. This study aims to evaluate the stiffness supplied by the intermediate web-post to the adjacent opening quarter through the coefficient k_θ depending on the geometrical parameters of the sinusoidal opening (Fig. 10).

3.2 Evaluation of the semi-rigid restraint/ Problem definition

The experimental studies led on the web-post specimens (Fig. 10(a)) showed that this specimen represents well the failure modes observed in the whole cellular beam. It has been observed that the failure modes obtained for the majority of the specimens detailed in the reference (Durif *et al.* 2013a, b) are close to that observed on the full scale beams with the same opening configurations. Furthermore, those studies allowed validating a second finite element model developed on the software CAST3M (Durif *et al.* 2013a). This software uses also four nodes shell elements and considers material and geometrical non linearities with high displacements. It has been decided to use this software because it provides a procedure for the calculation of the buckling eigenmodes that are useful to evaluate the elastic stiffness.

The study developed hereafter aims at defining the boundary conditions of an isolated quarter of opening in order to represent the behavior of the equivalent quarter that is tested in the conditions of the isolated web-post described in Fig. 10(a). The main goal is to define the elastic rotational restraint of the web-post on the analyzed panels of the sinusoidal opening (k_θ in Fig. 9).

The numerical model developed on CAST3M is used in this paper as a basis for a parametric analysis. The parametric study aims at evaluating the coefficient k_θ of the isolated quarter model (Fig. 9) depending on the opening geometric parameters a_0 (opening height), l_s (length of the sinusoidal part) and w (web-post width) (see Fig. 11). In the tested specimen, with some geometrical configurations, the analyzed local buckling of the sinusoidal part can interact with the global buckling of the intermediate web-post. Thus, a transversal stiffener is disposed at the mid

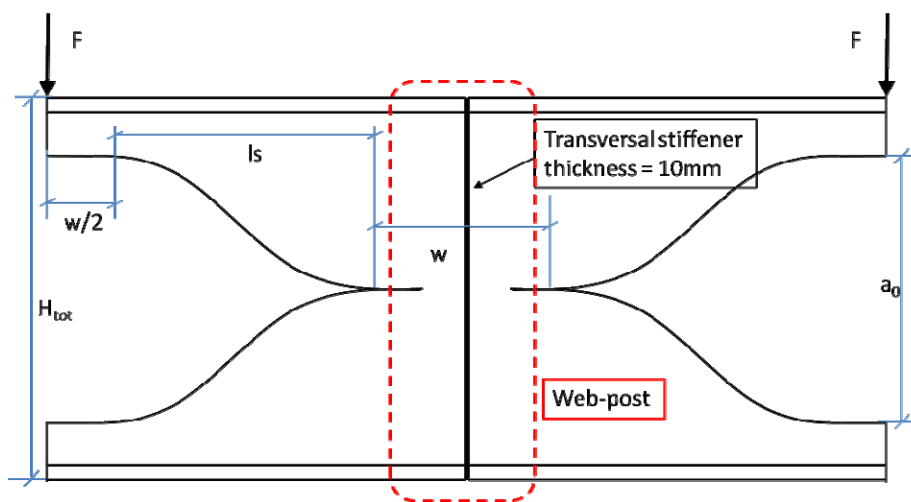


Fig. 11 Geometrical parameters considered for the isolated web-post

length of the intermediate web-post to prevent the global instability with a limited influence on the rotational restraint of the support (see Fig. 11).

3.3 Method of analysis

The study is based on the calculation of the elastic buckling loads using the procedure FLAMBAGE of the finite element software CAST3M. This procedure enables performing elastic buckling calculation. It is based on solving an eigenvalue problem that describes the buckling behavior of plates using shell elements. It seeks the eigenvalues that correspond to the critical loads for different buckling modes (CEA 2012).

This procedure calculates the conventional constant small deformation stiffness matrix K_E and the geometrical stiffness matrix K_σ associated with the stress field. This second matrix K_σ is proportional to the stress level and is used with an initial stress level σ_0 . El-Sawy and Nazmy (2001) described in detail the principles of the method that enables to recover the buckling loads and shapes through the eigenvalue problem resolution defined by the Eq. (8)

$$|K_E + \lambda K_\sigma(\sigma_0)| = 0 \quad (8)$$

When Eq. (8) is solved, it provides the eigenvalues λ , which correspond to the critical stress levels represented as $\sigma_{cr} = \lambda\sigma_0$ at which the corresponding buckling modes occur. The associated scaled displacement vectors define the mode shapes. The lowest eigenvalue defines the first buckling mode, which is used in the present study. The initial state of stress is induced by unit load F applied on both opening quarters (see Fig. 10(a)) and a unit load V applied on the isolated quarter (see Fig. 10(b)).

The buckling load V_{cr} of the isolated quarter model increases with the rotational restraint coefficient k_θ . The load configuration of the opening quarter in both geometrical models of isolated web-post and isolated quarter are the same. Consequently, the buckling load for the opening quarter in both models can be compared. Thus, by comparing the critical load of the isolated web-post model with that of the isolated quarter, the coefficient of elastic restraint applied on the isolated quarter model can be calibrated to represent the stiffness of the equivalent opening quarter in the configuration of isolated web-post.

This approach gives the possibility to evaluate the effect of the initial rotational stiffness, depending on the geometrical parameters of the opening, excluding the influence of the material yielding or the combination of large displacement and yielding. The determination of the rotational restraint coefficient (k_θ) follows three steps. Firstly, the critical load of the first buckling mode is calculated for the isolated web-post specimen (see Fig. 12(a)) to obtain the critical load coefficient called K_{cr1} . Secondly, the same calculations are done for one isolated quarter (see Fig. 12(b)) varying the k_θ value to obtain the critical force coefficient of the quarter K_{cr2} . The isolated quarter is considered pinned on the support line (see Fig. 7) with elastic rotational restraint coefficient k_θ . The value of k_θ considered for the isolated quarter is the one checking the equality $K_{cr2} = K_{cr1}$. Examples of first buckling modes for the web-post specimen with transversal stiffener and the corresponding sinusoidal isolated quarter are shown in Fig. 12.

Table 1 presents the results of a parametric study on the influence of the parameter ls on the value of k_θ . The other geometrical parameters (a_0 and w) remain constant to evaluate the influence of only one parameter. The parent profile is an IPE 450 corresponding to the tested profile. The cutting process of the cellular beam implies that the final beam height is $H_{tot} = 450 + a_0/2$.

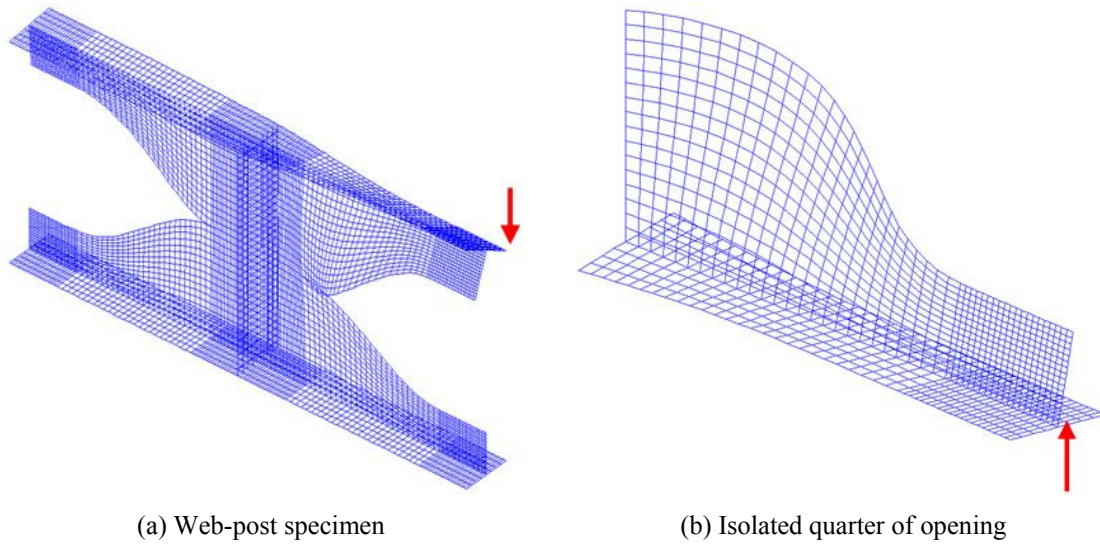
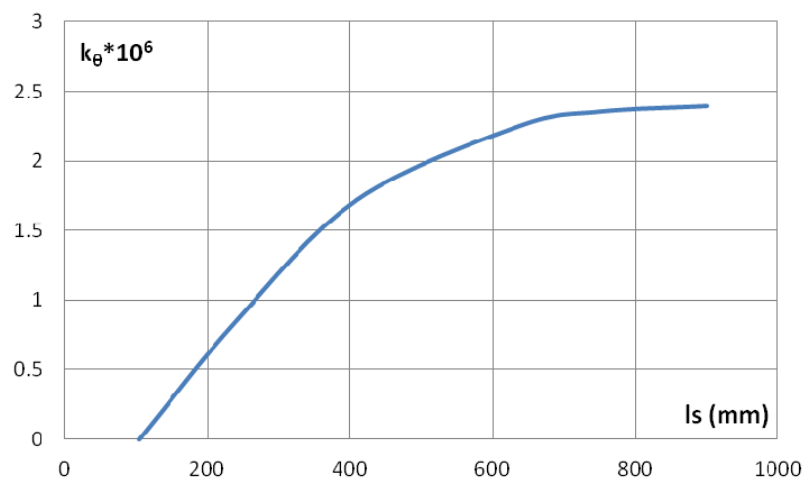


Fig. 12 Example of the first buckling mode for both studied models

Table 1 Influence of the parameter ls on the rotational restraint k_θ

Specimen n°	ls (mm)	a_0 (mm)	w (mm)	$K_{cr2} = K_{cr1}$	$k_\theta \times 10^6$ [N.mm/°]
1	900	450	205	1047.	2.39
2	750	450	205	1270	2.35
3	638	450	205	1495	2.25
4	410	450	205	2246	1.72
5	240	450	205	3300	0.847
6	105	450	205	4967	0

Fig. 13 Influence of the sinusoid length on k_θ [N.mm/°]

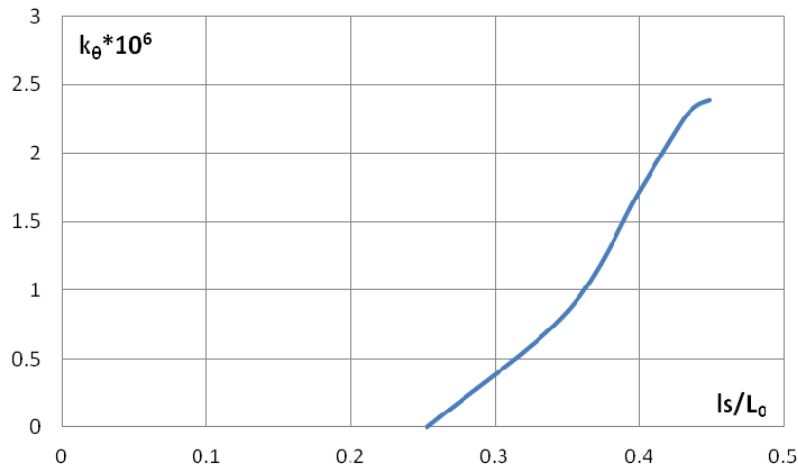


Fig. 14 Influence of the ratio ls/L_0 on k_θ [N.mm/°]

The curves shown in Figs. 13 and 14 illustrate respectively the evolution of the rotational stiffness k_θ (from Table 1) versus the sinusoidal part length (ls) and the dimensionless ratio ls/L_0 where L_0 is the opening length defined as $L_0 = 2 \times (ls + w/2)$. Those figures show that the influence of the ratio ls/L_0 on the value of k_θ can be approximated as a straight line (see Fig. 14). Thus, it is possible to define a linear relationship between k_θ and the ratio ls/L_0 . The same type of analysis can be performed with each of the two other geometric parameters (ls , a_0). However, varying two or three parameters imply that the response is a surface and the interaction between two parameters can be influential. Consequently, to establish a model predicting the value of k_θ based on the three selected parameters, it is necessary to use more appropriate tools. In this study, the theory related to the design of experiments is chosen (Pillet 2001, Cheng *et al.* 2012).

4. Design of experiments

Generally the objective of a design of experiment is to optimize the number of experiments that are necessary to identify the effect of different factors on a system. Furthermore, it can provide a good tool to define the experiments that are useful for developing simple analytical models which should predict the response of a system in function of the main influential parameters. The designs of experiments (DOE) are used in the literature for the prediction or the optimization of mechanical or structural problems (Madadi *et al.* 2012, Audebert *et al.* 2012). In this study, the approach is used to develop a formula predicting the influence of the rotational restraint of the intermediate web-post on the sinusoidal panels of the opening quarter in function of the opening geometrical parameters. The opening is characterized by its height (a_0) and its length ($L_0 = ls + w$) (see Fig. 11).

Therefore, three independent factors are studied: the opening height (a_0), the sinusoidal length (ls) and the flat part (w). The web-post width is equal to the flat part (w). In fact, the response of the system can either be influenced by each parameter separately or in interaction with the other parameters. The choice has been to use a full factorial design, which means that all combinations possible between the three parameters have to be led in order to get the influence of each

parameter and their interactions (Pillet 2001, Audebert *et al.* 2012). After developing the mathematical model it is possible to study the influence of the interaction terms. In order to perform the desired objective, the present investigation has been planned in the following sequence (Balasubramanian *et al.* 2008a, b).

- Step 1 : identifying the important parameters that have an influence
- Step 2 : finding the range of validity for each parameter (see §4.1)
- Step 3 : developing the experimental (numerical) design matrix (see §4.2)
- Step 4 : conducting the numerical tests described by the design matrix (see §4.2)
- Step 5 : developing the mathematical model (see §4.3)
- Step 6 : checking the adequacy of the developed model (see §4.4)

The main goal of this study is to define the rotational restraint provided by the intermediate web-post to the adjacent opening quarter based on the opening geometrical characteristics a_0 , w and l_s . Consequently, the thicknesses of the web and the flange and the height of the parent profile remain constant and equal to the dimensions of an IPE 500 profile. The choice of using an IPE 500 profile is motivated by the large range of opening sizes that can be made. The most important step before doing the parametric study is to correctly define the range of validity for each parameter.

To remain in the scope of the study, for all the tested configurations, the isolated quarter specimen (Fig. 10) has to be always representative of the behavior of the isolated web-post specimen (Fig. 11). This condition implies that the first buckling mode of the isolated web-post concerns the local buckling of the quarter of opening. It has been decided to calibrate the extreme values for each parameter in order to obtain the expected buckling mode.

4.1 Range of validity for each parameter

In order to define the range of validity for each parameter, the main condition is the representativeness of the isolated quarter specimen for the isolated web-post buckling mode. The isolated quarter considers an out of plan support at the support line which corresponds to the junction with the intermediate web-post. Thus, dimensions of isolated web-post with a global out of plan displacement of the intermediate web-post are not considered in the study. The limits proposed for each parameter are based first on the design practice. The cases studied called levels are given in Table 2 where the lower and upper limits of each parameter are named 1 and 3, and the mean value of these levels are named 2.

A parametric study varying the three parameters reveals that, for some cases, the isolated quarter specimen is not well representative of the isolated web-post specimen. In some cases the buckling mode of the isolated web-post combines local instability in the sinusoidal part and in the intermediate web-post. It has been observed that all those cases correspond to specific opening configurations, with maximum opening height with small sinusoidal length in comparison with the

Table 2 Values of the studied parameters with the limits

Level	a_0	l_s	w
1	250	200	200
2	445	515	480
3	640	830	760

Table 3 Critical loads of the isolated web-post and the isolated quarter

Config.	l_s (mm)	w (mm)	K_{cr1}	K_{cr2} with $k_\theta = 0$	Out of plan displ. of web-post
A	200	760	1856.2	1952.3	yes
B	200	650	2105.6	2172.4	yes
C	200	600	2243.5	2289.3	yes
D	250	600	2097.2	2037.0	yes
E	300	600	1963.6	1829.9	no

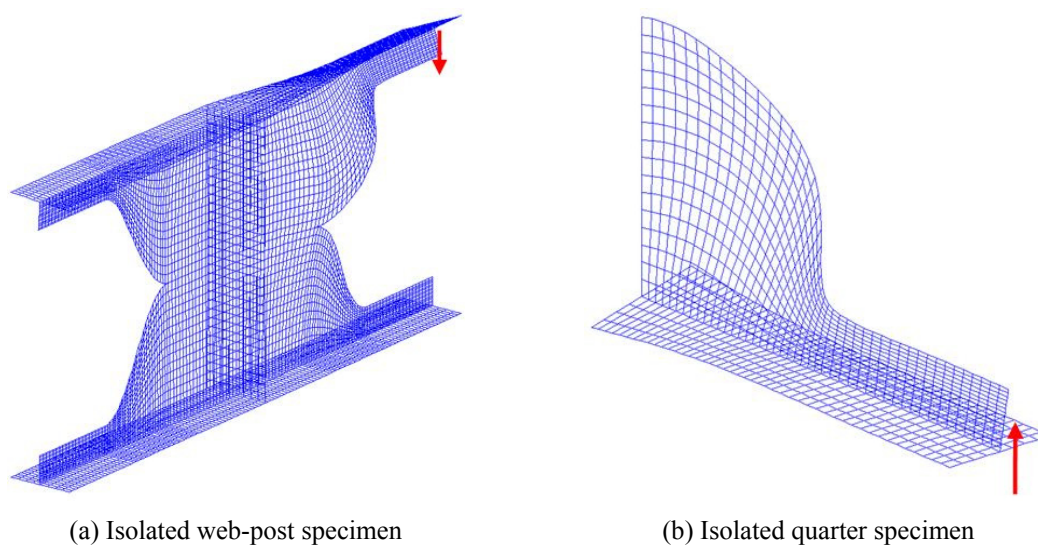


Fig. 15 First buckling modes of the configuration E (Table 3)

Table 4 Values of the chosen parameters

Level	a_0 (mm)	l_s (mm)	w (mm)
1	250	300	200
2	445	565	400
3	640	830	600

flat part length. However for all those cases, the errors on the values of K_{cr2} remain in the range of 5%. In the study, to keep the representativeness of the isolated quarter regarding the buckling mode, it has been chosen to modify the upper and lower limits for some parameters

The Table 3 presents the results of the parametric study led on the extreme values of the studied parameters. It can be observed in general that, when the intermediate web-post exhibits a modal out of plan displacement, the critical force coefficient K_{cr1} is lower than that of the isolated quarter K_{cr2} without any rotational restraint (see configurations A, B and C of Table 3).

The Fig. 15 describes the deflected shapes of the isolated web-post and the isolated quarter. It can be observed that there is no out of plan displacement of the intermediate web post. Furthermore, a rotational restraint has to be used in the isolated quarter to obtain the same critical

force coefficient as its reference web-post specimen. Therefore, the buckling mode of the quarter is representative of the isolated web-post qualitatively and quantitatively for the configuration *E* of the Table 3. Thus, the values of w and l_s in the configuration *E* are used as limit values in the parametric study. Table 4 gives the values chosen of the three levels for the studied factors which define the range of applicability of the developed mathematical model.

It can be noted that the range used for each opening parameter remain enough large to represent an important variety of opening configuration for sinusoidal openings for a parent profile IPE 500 which enables a large range of opening sizes. As the framework of the study is clearly defined, the parametric study can be performed.

4.2 Developing and conducting the parametric study

The Table 5 describes the full factorial design used in the study. The three levels for each factor, chosen to get an accurate model, are described in the Table 4. A study with two levels implies a linear interpolation between the two values which can lead to a less accurate model (Pillet 2001). The Table 5 presents the results of the parametric study and gives the value of the critical force coefficients ($K_{cr2} = K_{cr1}$) for each test and the value of the rotational restraint of the isolated quarter specimen representing the behavior of the web-post specimen.

4.3 Mathematical model development

The Table 5 presenting the results of the parametric study corresponds to a list of results that give the value of the output value Y for a set of operating conditions (factors). The objective of this part is to use those results in order to develop a polynomial law allowing the determination of the output value. This output is the rotational restraint depending on the input parameters that are the opening height a_0 , the sinusoidal length l_s and the web-post width w . The polynomial models are empirical models which are not directly linked to the observed phenomenon. Three response surface models are considered, the linear model, the pure quadratic model and the full quadratic model defined by the Eqs. (9)-(11) (Le 2012).

The polynomial model of first degree (linear)

$$Y_1 = \alpha_0 + \alpha_1 \alpha_0 + \alpha_2 l_s + \alpha_3 w \quad (9)$$

The polynomial model of second degree (quadratic):

$$Y_2 = \alpha_0 + \alpha_1 \alpha_0 + \alpha_2 l_s + \alpha_3 w + \alpha_{11} \alpha_0^2 + \alpha_{22} l_s^2 + \alpha_{33} w^2 \quad (10)$$

The polynomial model of second degree (quadratic with interaction terms)

$$Y_3 = \alpha_0 + \alpha_1 \alpha_0 + \alpha_2 l_s + \alpha_3 w + \alpha_{11} \alpha_0^2 + \alpha_{22} l_s^2 + \alpha_{33} w^2 + \alpha_{12} \alpha_0 l_s + \alpha_{13} \alpha_0 w + \alpha_{23} l_s w \quad (11)$$

The unknown coefficients “ α_i ” are obtained from the values of tests by a calculus of multi-linear regression using the response surface method known as the criterion of least-square. The resolution method gives the value of each coefficient α_i for each polynomial model in Eqs. (9) to (11). The coefficients α of the 3 models of response surface are exposed in the Table 6.

Table 5 Results of the parametric study

N°	a_0	ls	w	$K_{cr1} = K_{cr2}$	$k_\theta \times 10^6$ [N.mm/°]
1	1	1	1	3970	2.37
2	1	1	2	2864	1.54
3	1	2	1	2297	3.39
4	1	2	2	1807	2.07
5	1	1	3	2208	1.10
6	1	2	3	1495	1.49
7	1	3	1	1535	3.57
8	1	3	2	1276	2.10
9	1	3	3	1102	1.51
10	2	1	1	3727	1.58
11	2	1	2	2695	1.00
12	2	2	1	2213	2.85
13	2	2	2	1756	1.87
14	2	1	3	2079	0.65
15	2	2	3	1451	1.32
16	2	3	1	1499	3.28
17	2	3	2	1251	2.06
18	2	3	3	1078	1.47
19	3	1	1	3521	1.11
20	3	1	2	2542	0.61
21	3	2	1	2129	2.29
22	3	2	2	1702	1.56
23	3	1	3	1964	0.31
24	3	2	3	1406	1.07
25	3	3	1	1459	2.86
26	3	3	2	1225	1.92
27	3	3	3	1053	1.36

4.4 Application and validation of the mathematical model

The Fig. 16 shows the results of the relative differences between the three mathematical models using the coefficient of the Table 6 and the FEM results of the Table 5.

The Fig. 16 shows that the full quadratic model is the more accurate as its results are very close to those of the FEM. The relative differences for the linear model and the pure quadratic model are relatively high in some cases. This comparison emphasizes that the interaction terms could not be neglected, therefore a full factorial design is necessary to study a so complex behavior. The full quadratic model can be considered reliable considering the values that were used for calibrating the model coefficients with acceptable error due to the multi-linear regression. However, in order to validate the mathematical model, new test is done with values of the factors inside the range of

validity but different from the values previously used to calibrate the coefficients of the model. The Table 7 describes the three configurations chosen to validate the model.

The Table 7 gives the differences between the three mathematical models and the FEM results. It can be observed that for the three configurations tested, the more stable model remaining close to the FEM results is the full quadratic model. Furthermore, it can be seen that the linear or pure quadratic models give less accurate results for extreme values of geometrical parameters. Those simple examples reveal again that the interactions are important in order to get a model enough accurate. Finally, the full quadratic model allows getting a reliable and realistic value of the elastic rotational restraint coefficient in function of the opening geometrical parameters.

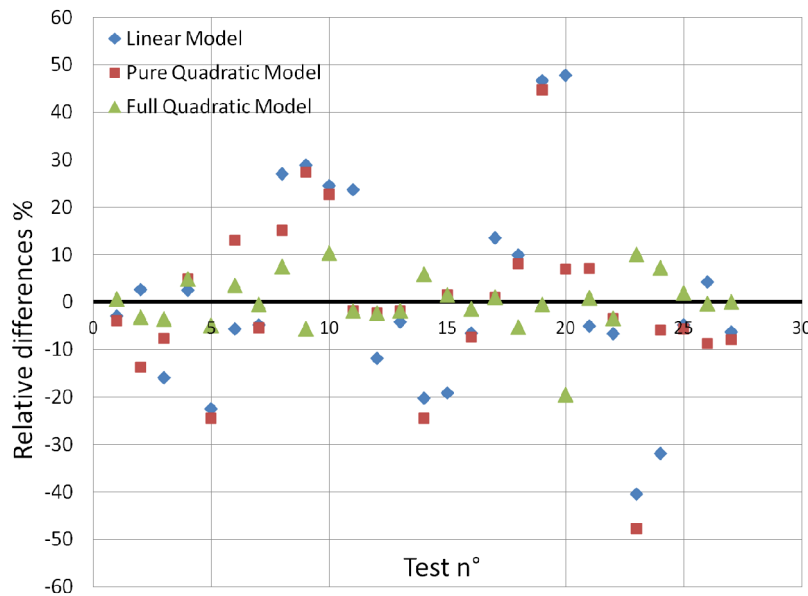


Fig. 16 Difference between the mathematical models and the FEM results

Table 6 Values of the coefficients a_i for the three mathematical models

Coefficient	Linear model ($\times 10^6$)	Pure quadratic model ($\times 10^6$)	Full quadratic model ($\times 10^6$)	Factor
a_0	2.832	2.451	3.048	1
a_1	-0.001723	-0.001847	-0.005072	a_0
a_2	0.00207	0.006898	0.006987	ls
a_3	-0.3613	-0.008168	-0.007691	w
a_{11}		1.388×10^{-7}	1.388×10^{-7}	a_0^2
a_{22}		-4.273×10^{-6}	-4.273×10^{-6}	ls^2
a_{33}		5.694×10^{-6}	5.694×10^{-6}	w^2
a_{12}			3.135×10^{-6}	$a_0 \times ls$
a_{13}			3.635×10^{-6}	$a_0 \times w$
a_{23}			3.709×10^{-6}	$ls \times w$

Table 7 Differences between the mathematical models and the FEM

a_0 (mm)	l_s (mm)	w (mm)	FEM k_θ (N.mm/°)	Relative difference %		
				Linear model	Pure quadratic model	Full quadratic model
500	500	300	2.035	5.60	1.47	4.20
500	400	500	1.0853	8.66	9.98	5.10
350	700	500	1.716	-9.03	-10.49	-3.21

5. Conclusions

The first observations made on the behavior at failure of cellular beams composed of sinusoidal openings allowed to point out that the Vierendeel bending can generate a local buckling of the most stressed opening sinusoidal panel. In order to study in more details this phenomenon, experimental and numerical studies have been performed on specimens taken from a cellular beam. This simpler specimen allows analyzing the local buckling of the quarter of opening for a given load similar to the Vierendeel bending.

The studied specimens allowed evaluating the influence of the intermediate web-post on the failure mode of the opening quarter panel. Indeed, the intermediate web-post has an important impact on the panel stiffness and on the stability of the adjacent sections composing the opening quarter. The main goal of the work presented in this paper has been to reveal the existence of an elastic rotational restraint between the intermediate web post and the opening quarter panel. It showed that this restraint can be represented by a simple coefficient of rotational restraint in an isolated quarter specimen.

In order to evaluate the stiffness provided by the intermediate web-post to the adjacent opening panel, two geometrical configurations of opening quarters have been studied and compared through a FEM elastic buckling analysis. The comparison of the buckling load between the two configurations (isolated quarter or with intermediate web-post) allowed calibrating the coefficient k_θ so as to evaluate the rotational restraint provided by the intermediate web-post. Furthermore, a study on the range of applicability of this comparative study has been carried out to validate the similarity of the two configurations regarding the failure modes.

Then, a method has been proposed and described in order to develop a polynomial law capable of quantifying this coefficient of rotational restraint. This law has been developed through a parametric study done on the geometrical opening parameters a_0 , l_s and w and the response surface method. The parametric study has been led according to a full factorial design in order to take in account every interaction terms between the different studied factors. It has been shown that those interaction terms cannot be neglected to obtain accurate prediction of the rotational restraint coefficient k_θ .

This coefficient k_θ is useful to develop realistic analytical model representing the buckling strength of the panels around the sinusoidal openings. By considering more realistic boundary conditions, a new criterion of stability can be developed to define more realistic section resistance in the case of sinusoidal openings. This can be performed by proposing a new calculation of the critical stress coefficient k_σ for the different tee sections along the opening quarter length so as to consider more realistic rotational restraints and out of plan supports.

The study presented in this paper aimed at proposing a simple method to justify analytical expression for a rotational restraint coefficient. This application of the design of experiments led to

reliable results and permitted to better understand the local buckling resistance of various configurations of openings. The approach developed in this study can be generalized to various ranges of parent profiles to get larger database and to develop a more general model predicting the buckling resistance of sinusoidal openings.

Acknowledgments

This paper has been prepared as a result of a research carried out at Blaise Pascal University for the completeness of a Ph.D. degree. The authors would like to thank the Ministry of Research for the scholarship and Arcelor Mittal group for the financial support and the supply of steel specimens for the experimental tests.

References

- Audebert, M., Dhima, D., Taazount, M. and Bouchair, A. (2012), "Behavior of dowelled and bolted steel-to-timber connections exposed to fire", *Eng. Struct.*, **39**, 116-125.
- Balasubramanian, M., Jayabalan, V. and Balasubramanian, V. (2008a), "Developing mathematical models to predict tensile properties of pulsed current gas tungsten arc welded Ti-6Al-4V alloy", *Mater. Des.*, **29**(1), 92-97.
- Balasubramanian, M., Jayabalan, V. and Balasubramanian, V. (2008b), "Developing mathematical models to predict grain size and hardness of argon tungsten pulse current arc welded titanium alloy", *J. Mater. Process. Tech.*, **196**(1-3), 222-229.
- CEA (2012), CAST3M Website, Last visit on July 2012. URL: <http://www-cast3m.cea.fr>
- Cheng, S., Miao, J. and Wu, S. (2012), "Investigating the effects of operational factors on PEMFC performance based CFD simulations using a three-level full factorial design", *Renew. Energ.*, **39**(1), 250-260.
- Chung, K.F., Liu, T.C.H. and Ko, A.C.H. (2001), "Investigation on Vierendeel Mechanism in steel beams with circular web openings", *J. Constr. Steel Res.*, **5**(57), 467-490.
- Darwin, D. (2003), Design of Steel and Composite Beams with Web Openings, Design Guide 2, (3rd Edition), AISC, 65 p.
- Durif, S. (2012), "Mechanical behavior of cellular beams with sinusoidal openings-development of an adapted analytical model", Ph.D. Thesis, Blaise Pascal University, Clermont-Ferrand, France. [In French]
- Durif, S., Bouchair, A. and Vassart, O. (2013a), "Experimental and numerical evaluation of web-post specimen representing the cellular beams with sinusoidal openings", *Eng. Struct.*, **59**, 587-598.
- Durif, S., Bouchair, A. and Vassart, O. (2013b), "Experimental and numerical modeling of cellular beams with sinusoidal openings", *J. Constr. Steel Res.*, **82**, 72-87.
- El-Sawy, K.M. and Nazmy, A.S. (2001), "Effect of aspect ratio on the elastic buckling of uniaxially loaded plates with eccentric holes", *Thin-Wall. Struct.*, **39**(12), 983-998.
- EN 1993-1-1 (2003), Eurocode 3 – Design of steel structures – part 1-1: General rules for buildings.
- ENV 1993-1-1 (1995), Design of steel structures – Part 1-1: General rules and rules for buildings, Annex N.
- Gandomi, A.H., Tabatabaei, S.M., Moradian, M.H., Radfar, A. and Alavi, A.H. (2011), "A new prediction model for the load capacity of castellated steel beams", *J. Constr. Steel Res.*, **67**(7), 1096-1105.
- Johansson, B., Macquois, R., Sedlacek, G., Müller, C. and Beg, D. (2007), "Commentary and worked examples to EN 1993-1-5: plated structural elements", JRC Scientific and Technical Reports.
- Kerdal, D. and Nethercot, D.A. (1984), "Failure modes of castellated beams", *J. Constr. Steel Res.*, **4**(4), 295-315.
- Lagaros, N.D., Lemonis, D.P., Papadrakakis M. and Panagitou, G. (2008), "Optimum design of steel structures with web openings", *Eng. Struct.*, **30**(9), 2528-2537.

- Lawson, R.M. and Hicks, S.J. (2005), "Developments in composite construction and cellular beams", *Steel Compos. Struct., Int. J.*, **5**(2), 193-202.
- Lawson, R.M., Lim, J., Hicks, S.J. and Simms, W.I. (2006), "Design of composite asymmetric cellular beams and beams with large web openings", *J. Constr. Steel Res.*, **6**(62), 614-629.
- Le, K.T. (2012), "Identification of random characteristics of embankments from the health monitoring of structures: application to port structures", Ph.D. Thesis, Faculté des Sciences et des Techniques, Université de Nantes, Nantes, France. [In French]
- Madadi, F., Ashrafizadeh, F. and Shamanian, M. (2012), "Optimization of pulsed TIG cladding process of satellite ally on carbon steel using RSM", *J. Alloy Compd.*, **510**(1), 71-77.
- Nadjai, A., Vassart, O., Ali, F., Talamona, D., Allam, A. and Hawes, M. (2007), "Performance of cellular composite floor beams at elevated temperatures", *Fire Safety J.*, **42**(6-7), 489-497.
- Pillet, M. (2001), *Experimental Design by the TAGUCHI Method (Les plans d'expériences par la méthode Taguchi)*, (3rd Edition), Organisation (Groupe Eyrolles), Paris, France. [In French]
- Redwood, R.G. (1978), "Analysis and design of the beams with web openings", *Revue Construction Métallique*, **3**, 15-27. [In French]
- Soltani, M.R., Bouchair, A. and Mimoune, M. (2012), "Nonlinear FE analysis of the ultimate behavior of steel castellated beams", *J. Constr. Steel Res.*, **70**, 101-114.
- Tsavdaridis, K.D. (2010), "Structural performance of perforated steel beams with novel web openings and with partial concrete encasement", Ph.D. Thesis, School of Engineering and Mathematical Sciences, City University, London, UK.
- Tsavdaridis, K.D. and D'Mello, C. (2011), "Web buckling study of the behavior and strength of perforated steel beams with different novel web opening shapes", *J. Constr. Steel Res.*, **67**(10), 1605-1620.
- Veljkovic, M., Johansson, B., Lawson, R.M., Hicks, S., Cajot, L.G., Vassart, O., Bureau, A., Feldmann, M., Müller, C. and Hechler, O. (2006), "Large web openings for service integration in composite floors", *CECA Projects*, 120 p.
- Ward, J.K. (1990), *Design of Composite and Non-Composite Cellular Beams*, The Steel Construction Institute Publication, UK, 100 p.